Structural Engineering and Mechanics, *Vol. 74, No. 1 (2020) 69-82*
DOI: https://doi.org/10.12989/sem.2020.74.1.069

Introducing a new all steel accordion force limiting device for space structures

Maryam Poursharifi[1a], Karim Abedi[*1], Mohammadreza Chenaghlou[1b] and Robert B. Fleischman[2c]

[1]*Faculty of Civil Engineering, Sahand University of Technology, Tabriz, Iran*
[2]*Department of Civil Engineering and Engineering Mechanics, School of Engineering, University of Arizona, 1209 E. 2nd St., Tucson, AZ 85721, United States*

(Received March 13, 2019, Revised October 8, 2019, Accepted November 12, 2019)

Abstract. A significant defect of space structures is the progressive collapse issue which may restrict their applicability. Force limiting devices (FLDs) have been designed to overcome this deficiency, though they don't operate efficiently in controlling the force displacement characteristics. To overcome this flaw, a new type of FLD is introduced in the present study. The "all steel accordion force limiting device" (AFLD) which consists of three main parts including cylindrical accordion solid core, tubular encasing and joint system is constructed and its behavior has been studied experimentally. To improve AFLD's behavior, Finite element analysis has been carried out by developing models in ABAQUS software. A comprehensive parametric study is done by considering the effective design parameters such as core material, accordion wave length and accordion inner diameter. From the results, it is found that AFLD can obtain a perfect control on the force-displacement characteristics as well as attaining the elastic-perfect plastic behavior. Obtaining higher levels of ultimate load carrying capacity, dissipated energy and ductility ratio can be encountered as the main privileges of this device. Ease of construction and erection are found to be further advantages of AFLD. Based on the obtained results, a procedure for predicting AFLD's behavior is offered.

Keywords: space structure; force limiting device; accordion; progressive collapse; FEA

1. Introduction

Space structures are the best solution for covering large areas with few or no intermediate supports. The most significant feature of these structures is their delicate appearance, ease of erection, light weight as well as being economic (Nooshin 1998). Despite these valuable advantages, some space structures are vulnerable to progressive collapse depending on their structural configuration, boundary conditions, applied loading as well as loss of key members. Progressive collapse mostly commence due to buckling of compression members which often possess brittle buckling behavior (Schmidt *et al*. 1976, Thornton and Lew 1984). Space structures are mostly used as roofing system for overcrowded sites such as airports and gyms; therefore their collapse can lead to great loss of lives and property. Accordingly, a variety of mechanisms have been developed over the years to prevent the progressive collapse and improve the double layer space structure's response. These mechanisms can be generally classified as force management and ductility management (Hanaor *et al*. 1989). Force management is based on controlling member's force distribution by appropriate design of geometric configuration. Diagonal member removal and utilizing eccentric diagonal members are the methods classified in this category. The basic idea behind the ductility management method is utilizing the reserve load carrying capacity inherent in ductile redundant systems. Two main methods in this category are under-designing the critical tension members and utilizing FLDs. Among the aforementioned methods, FLD is an effective tool for preventing the sudden buckling of compressive members, due to its dominant capability in obtaining constant load carrying capacity regardless of the influence of imperfections (Tada and Wakiyama 1993, Schmidt and Hanaor 1979). The basic idea behind this mechanism is applying FLD to critical compression members in order to modify the brittle post-buckling behavior of compressive members into the elastic-perfect plastic behavior with long plateau of member ductility, as shown in Fig. 1.

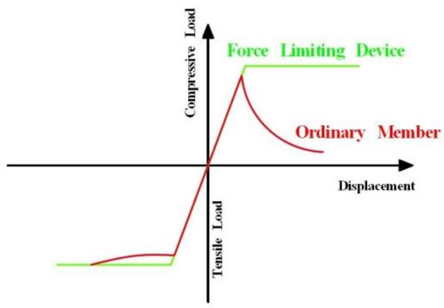

Fig. 1 FLD's behavior in comparison with behavior of ordinary members

*Corresponding author, Professor
E-mail: kabedi@sut.ac.ir
[a] Ph.D. student
E-mail: m_poursharifi@sut.ac.ir
[b] Professor
E-mail: mrchenaghlou@sut.ac.ir
[c] Professor
E-mail: rfleisch@email.arizona.edu

http://www.techno-press.com/journals/sem&subpage=7
ISSN: 1225-4568 (Print), 1598-6217 (Online)

The initial concept of FLD for preventing progressive collapse was presented by Schmidt and Hanaor (1979). The FLD was used for obtaining constant load carrying capacity in double layer space structures. In a subsequent work, Hanaor and Schmidt (1980) introduced two distinct types of FLD; hydraulic cylinder FLD and friction FLD. In the former, a hydraulic piston was included in the FLD which operated by exceeding the fixed pressure. The friction FLD which operated by moving a metal rod through a cutting tool, indicated better force-displacement behavior although it was complicated to obtain fixed limit load for this case. The multi-tubular FLD was introduced by Parke (1988). This FLD was consisted of two square hollow section tubes and four rectangular strips. The characteristics of this FLD were found to be dependent upon length and cross sectional area of the strips. This experimental work demonstrated that the multi tubular idea could efficiently improve the ductility of double layer grid space trusses, though it did not significantly recover the elastic force distribution inside grid. Mukai *et al*. (1993) experimentally inserted the multi tubular FLD to three small scaled grids. Their results showed that multi tubular FLD is a good mechanism for improving the load capacity and deformability of truss structure provided that FLD be fitted to the members with the largest compressive axial force as well as the members with compressive axial force close to the largest one. El-sheikh (1999) carried out a parametric study to investigate the effects of applying FLD on the behavior of double-layer trusses, considering different parameters such as truss configuration, aspect ratio and boundary conditions. Results indicated that effect of FLDs becomes more evident in corner supported space trusses. The applicability of FLD for handling the compression member buckling issue under transient wind load has been demonstrated in a numerical work by Bai *et al*. (2012). In this work, the Monte Carlo method combined with response surface approach was adopted to consider uncertainties related to wind load change rate and member imperfections under combined static and transient wind loading. It was observed that utilization of FLDs was helpful in reducing the failure probability of roof collapse under transient wind load. Subsequently, Bai *et al*. (2013) studied nonlinear dynamic behavior of steel roofs equipped with FLDs under transient up-lift wind pressure and showed that applying FLDs significantly reduces structure's deformation under upward wind load. In a more recent work, Shekastehband (2018) numerically investigated in to the effect of applying force limiting device on tensegrity space structures behavior. Results indicated that applying FLD to a small selection of members considerably improves the load carrying capacity and initial stiffness. It was also found that the effect of applying FLD becomes more noticeable as the number of supports decreases. The mentioned sophisticated versions of FLD are now available in the technical literature, each having its own cons and pros. Ineffective control of the force-displacement characteristics, is considered as the significant drawback of the aforementioned FLD versions. To this should be added the fact that they are not able in obtaining the ultimate load carrying capacity as well as achieving the elastic-perfect plastic behavior. For such reasons, investigation for improving the behavior of FLDs to overcome such flaws is highly required. In the present work, a new generation of FLD is introduced. The idea behind this new version of FLD's configuration is inspired by the all steel buckling restrained brace (BRB) and accordion metallic damper. It should be acknowledged that while the FLD mechanism is not a new one and dates back to 1979, improving the all steel BRB mechanism is absolutely an ongoing field. Buckling restrained braces have been widely used to provide the same load-deformation behavior in both compression and tension in braced frames. The concept of BRB is based on restraining the buckling of brace's core by encasing in order to achieve higher energy absorption capacity (Xie 2005). All steel BRBs are new generation of BRBs which benefit from ease of assembling, light weight and higher energy dissipation capacity. These advantages have stimulated the interest to optimize all steel BRB's configuration. There are plenty of studies which have been conducted on this field (Beiraghi 2017, Hemmati *et al*. 2018). Chou *et al*. (2016) came up with an idea about the sandwich BRBs, in which a core plate was sandwiched between two identical restraining members. Pandikkadavath and Sahoo (2015) conducted a study on the ductility demand of three story steel frame equipped with hybrid braces, consisting of a reduced length BRB and an elastic buckling-type brace. In a more recent work, Mirtaheri *et al*. (2018) applied numerical methods in order to optimize the steel core length in BRBs. In the field of grooved tubes, Hosseinipour and Daneshi (2003) experimentally studied the thin walled grooved tubes behavior, concluding that the buckling mode and energy absorption by axial force can be controlled by means of tube's groove geometry. In a more recent work, Motamedi and Nateghi (2018) studied the mechanical characteristics of accordion metallic damper. Results indicated that high energy absorption level and large deformation capacity was observed due to formation of plastic hinges in damper. It should be mentioned that in the aforementioned researches the accordion damper was a steel tube. However, the accordion core is a solid shaft in the device introduced in the present study. In the present study, taking advantage of BRB design principles, we introduce a new type of FLD which can overcome the serious defects of previous FLDs. Upgrading the past design of FLD with the modern technology of all steel BRB, leads to introducing the "all steel accordion force limiting device". The innovation of the proposed AFLD is related to the solid core's special shape which is designed to be accordion. Also equipping AFLD with encasing is considered as a novel innovation which prevents core from buckling. To reach this objective, the present work is organized as follows: we start with introducing the accordion force limiting device focusing on its detailed design. Next, we proceed with describing the experimental program including the manufacturing, assembling and testing procedures. Then, the experimental results are presented for two test samples. Principles for modeling AFLD with ABAQUS finite element software is next presented, followed by a comprehensive parametric study on AFLD's behavior. Finally, a procedure for predicting AFLD's behavior is suggested.

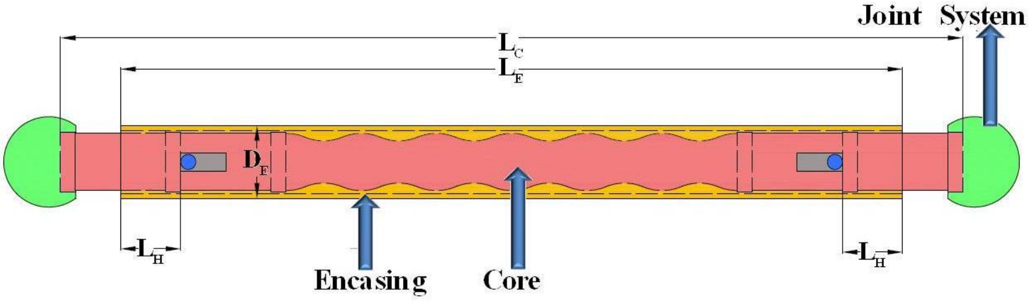

Fig.2 Schematic figure of AFLD

Table 1 The list of symbols and notations used in the present paper

D_e	Encasing diameter
D_c	Accordion diameter
D_{ci}	Inner diameter of accordion
D_{co}	Outer diameter of accordion
E	Elasticity modulus of encasing
F	Force
I	Moment of inertia
K	Encasing effective length factor
L_c	Core length
L_E	Encasing length
L_H	Distance between the hole and end of encasing
L_{cw}	Accordion wave length
P_e	Euler load
P_y	Yield load
t	Encasing thickness
α	Factor related to the accordion's curvature
β	Factor related to ability of encasing to prevent global core buckling
σ_y	Yield Stress

2. Accordion force limiting device

Accordion Force limiting device, proposed in the present study, is a newly developed generation of common FLDs. In comparison with ordinary FLDs, AFLD has enhanced characteristics in terms of force carrying capacity and ductility as well as providing constant load level. The most important feature of this soft member is that encasing acts as restraining system preventing the core from buckling. It is worth mentioning that, AFLD can be installed in double layer space trusses like the ordinary members and is compatible with all joint types. Being inspired by BRB configuration, AFLD is consisted of three main parts including cylindrical core, tubular encasing and joint system as shown schematically in Fig. 2. It is to be mentioned that the cylindrical core is not tubular and it is a solid shaft. As seen in this figure, the accordion shape core with length of L_c is located inside a tubular encasing with length of L_E and diameter of D_E. Two joints are placed at the two ends of core. Two assembling holes are drilled in a finite distance (L_H) from two ends of encasing to fix the core location inside the encasing. Slotted holes are considered to enable the free movement of core during the compression test. Bolt connection is used to connect encasing to core as well as spherical joint to core. By using bolt connections, AFLD can be assembled fast and disassembled easily. Furthermore, even after buckling of core, encasing can be used in other AFLDs.

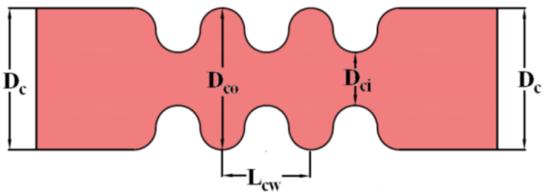

Fig. 3 Effective parameters in AFLD's core design

2.1 AFLD design

As mentioned before, AFLD is consisted of three main parts including core, encasing and joint system. In the following, the design principles of these items are described in detail. In order to be compatible with other members of space structure, the core shape was selected to be cylindrical and accordingly encasing shape was chosen to be tubular. Effective parameters in the design of AFLD's core are the inner diameter of accordion (D_{ci}), outer diameter of accordion (D_{co}), core diameter (D_c) and the accordion wave length (L_{cw}) as illustrated schematically in Fig. 3.

The outer diameter of accordion (D_{co}) depends upon encasing diameter and gap between core and encasing. Inner diameter of accordion (D_{ci}) should be chosen according to the ultimate load carried by AFLD. For a given core material and a determined force, the inner diameter of core is specified as:

$$D_{ci} = 2\sqrt{\frac{F}{\pi\sigma_y}} \tag{1}$$

Where, F refers to the critical force of AFLD and σ_y is the yield stress of core material. To design the tubular encasing, one should define the length, diameter and thickness of tube. The length of encasing is chosen according to the length of any critical compression member which will be replaced by the AFLD. The inner diameter of the encasing (D_E) is equal to the sum of cylindrical core diameter and a safe zone, say 1-2 mm, as steel core expands due to Poisson's effect while compressing. This gap is considered between core and encasing to minimize the friction and also prevent axial stress transition. To define tube thickness range (t), the Watanabe criterion has been applied. In order to prevent local and global buckling of encasing during core buckling, encasing dimensions should satisfy Watanabe criterion (Watanabe *et al*. 1988) as mentioned in buckling restrained braces, which is defined as:

$$\frac{P_e}{P_y} \geq 1.5 \tag{2}$$

In which, P_y is the yield load of core and P_e is the Euler buckling load of encasing; that is (Gere and Goodno 2012):

$$P_e = \frac{\pi^2 EI}{KL^2} \tag{3}$$

Where, E is the elasticity modulus of encasing, L is the total length of encasing, and K is the encasing effective length factor which is assumed to be one. The moment of inertia, I, for the encasing is defined to be:

$$I = \frac{\pi}{64}\left((D_{ei}+t)^4 - (D_{ei})^4\right) \tag{4}$$

As the last item in designing AFLD, now we mention the points regarding the joint system. Joints in space structures are utilized to join the members and transfer the force among them. The joint itself must resist design load in order to prevent joint failure. The AFLD is highly adaptable with all usual joints of space structures. For the proposed AFLD, we have decided to rely on Mero-like spherical joints, due to its high convenience in assembling as well as satisfying pin boundary conditions. These joints are similar to Mero system patented by the German company "MERO TSK". Mero joint which acts as a pin joint, is a spherical piece with threaded holes to which members connect. As the force range applied to AFLD has to exceed the critical force, the conical part of Mero-type joint is eliminated. That is to say that, AFLD is directly connected to the spherical joint. The connection between AFLD's core and Mero-type joint is provided by a high tensile bolt to transfer the axial compression force to joints.

3. Experimental program

Two tests were carried out to investigate AFLD's behavior under uniaxial compressive loading. The utilized materials for AFLD parts were selected and tested to identify their properties. The parts were manufactured by CNC machining and assembled to be tested by the AFLD test circuit. In the following, these items will be explained in detail.

3.1 AFLD Manufacturing

The CK45 steel as the core and joint system material has been selected due to its high strength, fine machinability and local availability. Upon deciding on the material, three coupon test specimens were fabricated (see Fig. 4-a) by machining the CK45 steel samples according to the DIN 50-125 standard. The tensile test was performed on coupon specimens by a tensile testing machine (Shimadzu Corp. Japan) equipped with clip-on extensometers to achieve material properties accurately. Results of tensile coupon tests, including Young modulus, yield stress, ultimate stress and elongation at necking, are given in Table 2. Encasing is designed to prevent the global buckling of core. It is worth noting that, the local buckling of core should also be prevented. In the proposed AFLD, seamless steel tube was used as the encasing material mostly due to its precise wall thickness and low friction of inner side. This type of tube was chosen to prevent the risk of welding problems, such as corrosion and weld decaying. In order to obtain the properties of encasing material, three coupon test specimens were prepared (see Fig. 4-b). Mechanical properties of encasing material are given in Table 3.

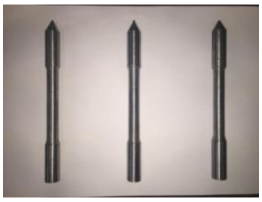

(a)

(b)

Fig. 4 Three coupon test specimens for; (a) core material, (b) encasing material

Table 2 Material properties of core material.

Specimen no.	Young modulus	Yield Stress	Ultimate stress	Elongation at necking
	(GPa)	(MPa)	(MPa)	(%)
1	195	396	650	24
2	194	385	652	24
3	195	385	654	25

Table 3 Material properties of encasing material.

Specimen no.	Young modulus	Yield Stress	Ultimate stress	Elongation at necking
	(GPa)	(MPa)	(MPa)	(%)
1	195.5	640	696	20
2	195	637	692	21
3	195	637	694	22

Once the core, joint system and encasing materials were selected and tested, the whole AFLD could be manufactured. It should be mentioned that two similar samples of AFLD were manufactured in the present work. The same design patterns have been adopted for the two cases and the only difference was in dimensions. Detailing of AFLD dimensions in first and second tests is shown in Fig. 5. To fabricate the core, encasing and joints of AFLD, the parts were all cut by CNC machine according to the dimensions shown in Fig. 5. For the case of spherical Mero-like joints, heat treatment was applied to increase their hardness. Once all the parts were fabricated, they were assembled to form AFLD. In order to minimize the friction between encasing and core, the core surfaces were

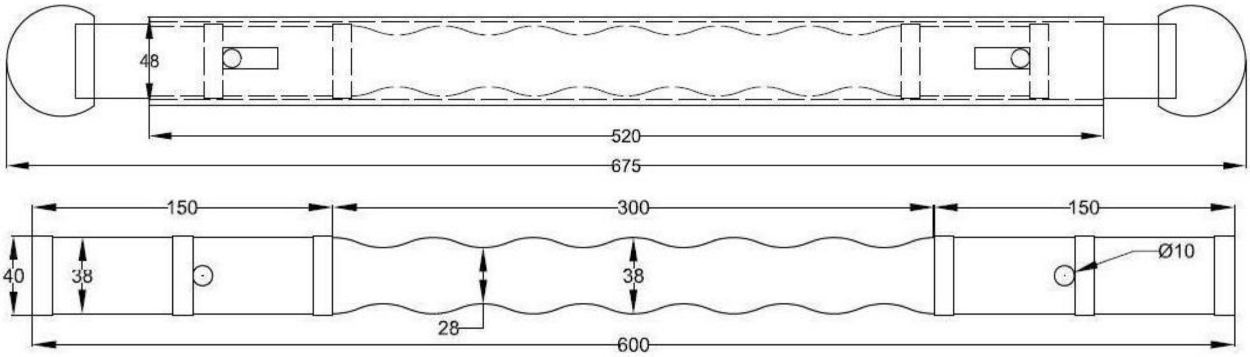

(a)

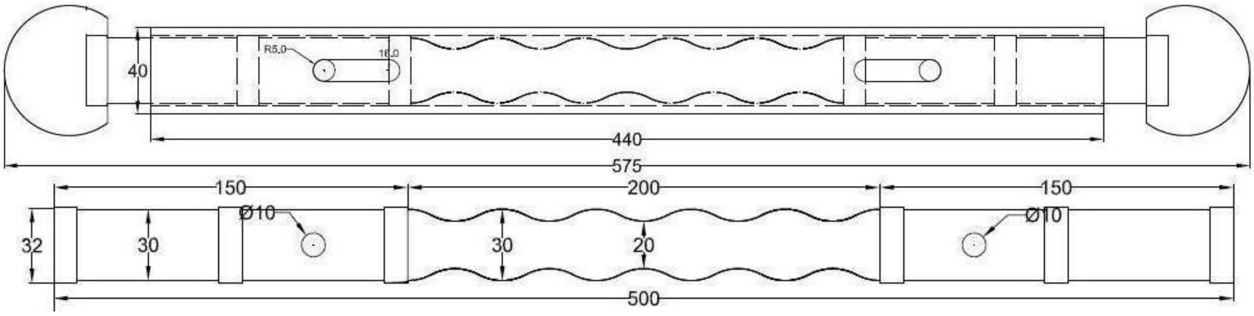

(b)

Fig. 5 Detailing of AFLD design (Unit: mm): (a) Test 1, (b) Test 2

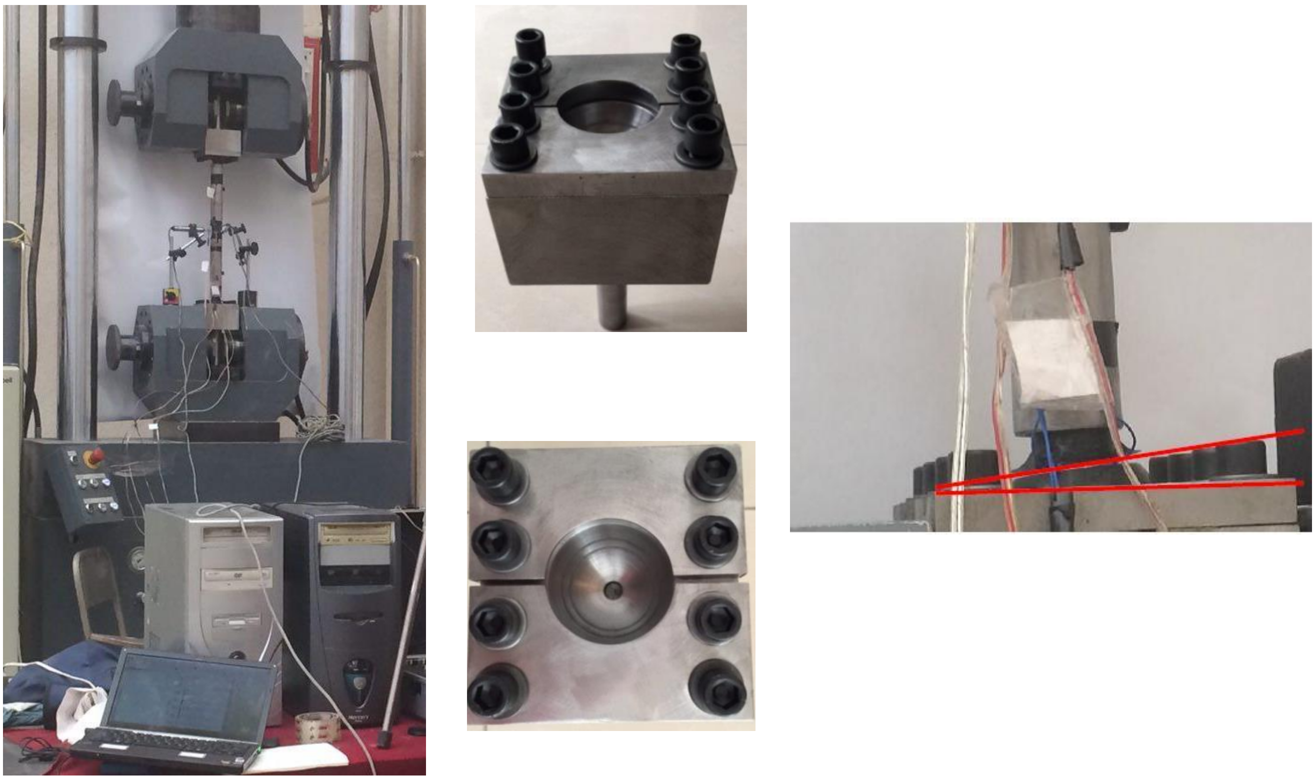

(a) (b) (c)

Fig. 6 Experimental test setup; (a) AFLD implanted in UTM device, (b) Auxiliary grip gadget, (c) Rotation of Mero-like spherical joint in auxiliary grip gadget

completely brushed with multi-purpose calcium-sulfonate grease prior to being placed inside the encasings. Core was then located inside the encasing followed by tightening the assembling bolts. In order to add the Mero-like spherical

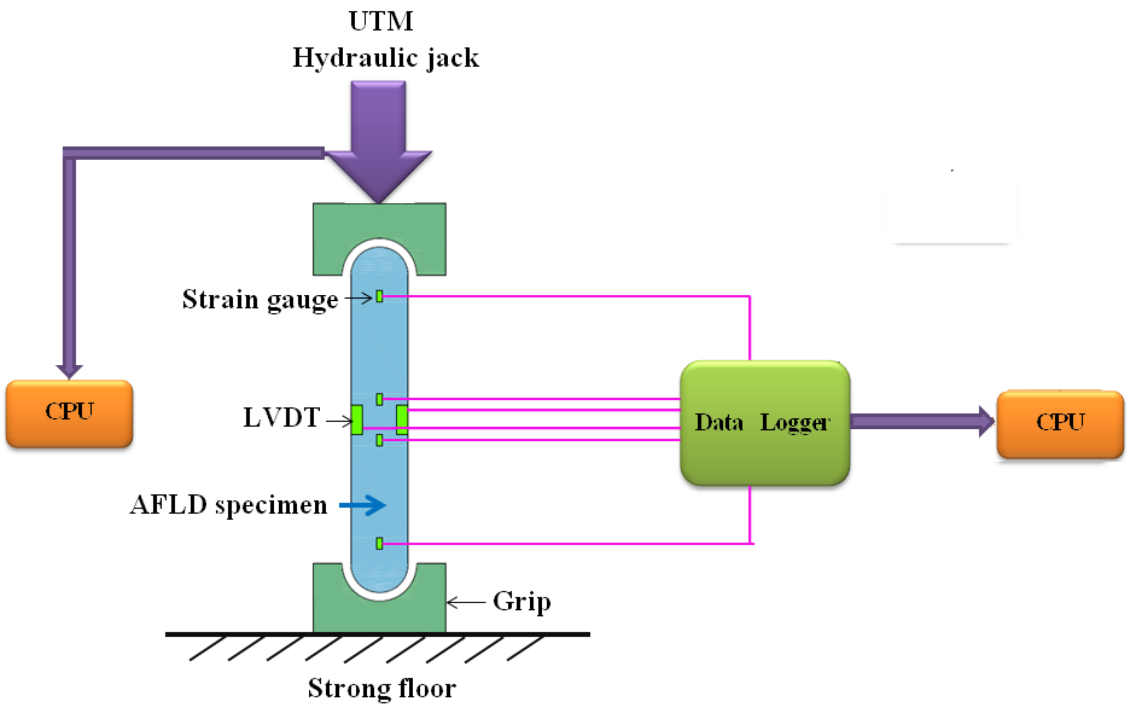

Fig. 7 Schematic depicting the AFLD test circuit

joints, two holes were drilled on two ends of core. The joints were then fixed to the core by bolts.

3.2 Loading and instrumentation

The test program covers uniaxial compressive tests on the two mentioned specimens implemented by universal testing machine (UTM). The UTM (ZwickRoell, Germany) in the structures laboratory of Sahand University of Technology was used to perform the tests. To test the AFLD specimen by UTM, it was fixed in two ends by pneumatic grips while the upper hydraulic jack exerted compressive force up to the range of 500 kN. Testing machine, AFLD specimen and the test setup prior to testing is shown in Fig. 6-a. It is worth noting that in the present study, the specimen was located inside an auxiliary grip gadget to be fixed between UTM grips. This auxiliary setup has been designed and manufactured to provide hinged joint boundary conditions. This segment has a hemisphere hole (see Fig. 6-b) in which the spherical joint is placed on a film of greasy lubricant, to allow rotation of AFLD's end part (Mero-like spherical joint) up to 20 degrees besides of restricting the axial displacement. The tests were carried out under displacement control method. Applied displacement rates in the first and second tests were set to be 0.02mm/s and 0.005mm/s, respectively. As mentioned before, accordion force limiting device is proposed to prevent progressive collapse in space structures which commence mostly due to buckling of compressive members. Therefore, the critical issue, which should be focused on it, is AFLD's behavior under compression loading. That is the reason for applying uniaxial compressive force on AFLD. It should be noted that this device is specialized for space structure and due to these structures low weight; they are not usually vulnerable in earthquakes. The magnitudes of applied load as well as the relative displacement (center to center) of Mero-like ball joints were recorded by the associated software of UTM. In order to measure the out of plane buckling deformation, Two LVDTs (linearly variable displacement transducers) were fixed in the middle of encasing, perpendicular to each other. Two 120 Ohm strain gauges were used in top and bottom of core and two 120 Ohm strain gauges were installed in the middle of encasing to measure strain. The data from strain gauges and LVDTs were collected every 0.1 second by data logger system connected to LVDTs and strain gauges. Magnitudes of applied force and relative displacement were recorded in each loading step. The schematic figure of AFLD test circuit is shown in Fig. 7.

4. Experimental results and discussion

In this section, we present the experimental results obtained for the AFLD behavior in the test circuit depicted schematically in Fig. 7. AFLD was loaded in compression and the axial force-axial displacement response was recorded by UTM. Fig. 8 shows the axial force-axial displacement response of the first test specimen (the specimen with dimensions shown in Fig. 5-a). Fig. 8 shows that yielding of core has initiated at the axial load level of 335kN corresponding to displacement of 2.2mm as pointed by letter A in this figure. In this test specimen, test was stopped at axial load level of 460kN before the failure of AFLD. The decision for stopping the test was taken to care the machine, as the universal testing machine started to vibrate at the load level of 430kN. The failure of AFLD was not observed at the end of test, as loading was stopped

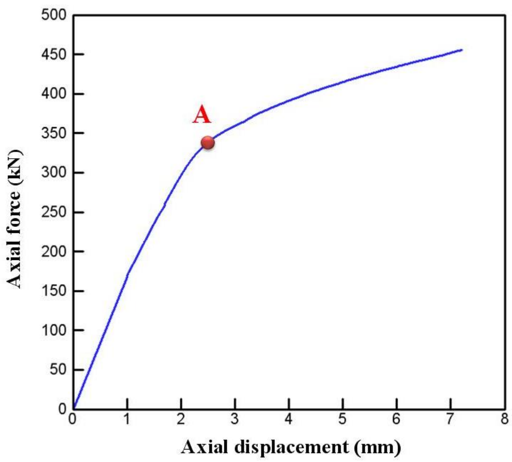

Fig. 8 The axial force-axial displacement response of the first test specimen Point A refers to the core yield initiation

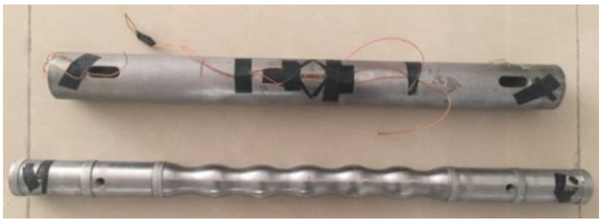

(a)

(b)

Fig. 9 Core and encasing at the end of test; (a) first specimen (b) second specimen

before this criterion. This has been clearly depicted in Fig. 9-a, which shows the core and encasing of first specimen were intact at the end of test. According to data obtained from LVDTs, the out of plane displacement in the middle of encasing is maintained equal to zero during test. The obtained data from the strain gauges located in top and bottom of encasing is coincident with the results of LVDTs. That is to say that, the global buckling has not occurred in the encasing.

Since for the case of first specimen, the adequate force could not be provided by UTM, we resorted to the second test specimen (the specimen with dimensions shown in Fig. 5-b). The second test specimen which was more slender in comparison with the first specimen, enabled the test procedure to proceed towards the collapse step. The axial force-axial displacement response of second test specimen is illustrated in Fig. 10. This figure shows that yielding started to occur at the axial load level of approximately 140 kN as pointed by letter A in this figure. Then, AFLD continued to carry compression load followed by formation of extra plastic hinges. In point B, all plastic hinges were formed and AFLD reached its ultimate loading capacity.

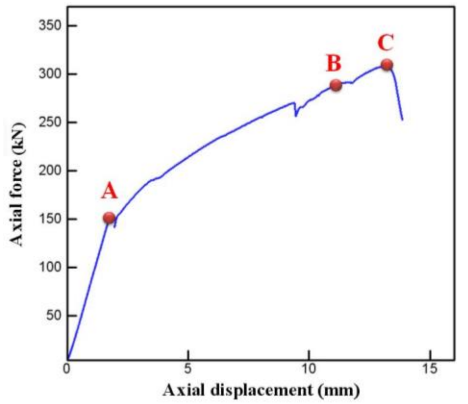

(a) Points A, B and C indicate the key behavior points of AFLD

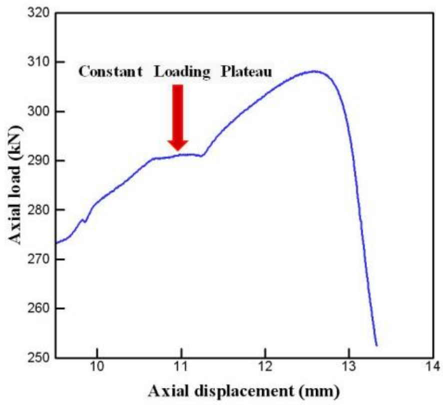

(b) Zoomed plot of Fig. 10 (a) indicating constant loading plateau

Fig. 10 The axial force-axial displacement response of the second test specimen

The constant loading plateau is obviously shown in Fig. 10. Subsequently, core met the encasing followed by increasing the load carrying capacity as will be addressed by LVDTs results. The excessive strength caused by encasing's confining effect on core is obviously visible in Fig. 10-a, as the curve continues its ascending path to reach point C.

In this point, due to excessive lateral displacement, encasing began to show out of plane buckling and the specimen started to collapse. Core and encasing of the second test specimen, at the end of test, are shown in Fig. 9-b. It can be seen in this figure that core and encasing experienced the first mode of buckling. Displacement-time response of second specimen obtained from perpendicular LVDTs is presented in Fig. 11. As shown in this figure, at the beginning of test, displacement of both LVDTs is approximately negligible. Therefore, the designed AFLD was capable in preventing the core buckling in the range of design load. The test was then continued to observe the failing mechanism. The results from LVDTs reveal that encasing started to participate in carrying the compression load, exactly after its deformation which is in accordance with the first buckling mode of core. After point B, rising in load caused AFLD to be in over strength state as the curve follows its path to reach point C. In this point, excessive lateral force exerted by core led to encasing's global buckling.

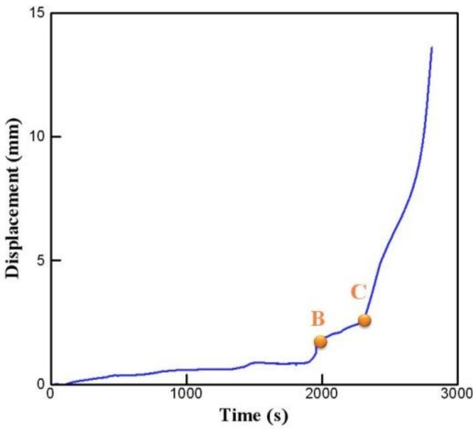

(a) first LVDT

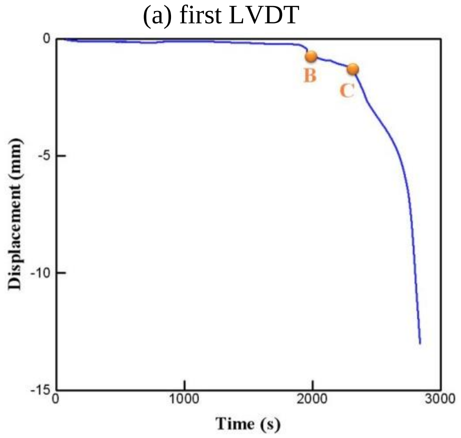

(b) second LVDT

Fig. 11 Displacement-time response of LVDTs. Points B and C refer to the formation of first and second plastic hinges

As explained in part 3.2., an auxiliary grip gadget was fabricated for the AFLD test. The main objective of this auxiliary set up was to enable free rotation of the Mero-like spherical joint up to a finite range so that the joint could act as a pin jointed member like the usual Mero joint members. The free rotation of the spherical joint during the test was observed, which can be clearly seen from Fig. 6-c, where the acute angle (shown by red colors in Fig .6-c) between the top plate of auxiliary gadget and the flat side of joint is visible. This fact implies that the designed auxiliary grip gadget operated properly. The experimental results clearly reveal that AFLD could successfully modify the brittle buckling state to elastic-perfect plastic behavior. Despite ordinary members in which the load carrying capacity has a sudden drop referred as brittle buckling (see Fig. 1), AFLD experienced no sudden drop in its load carrying capacity (as shown in Fig. 10-a) that means no brittle buckling has happened. This notion confirms that AFLD is the perfect device for improving the “brittle buckling” to “elastic-perfect plastic behavior”. The next advantage of AFLD seen in the experimental test is related to the intact status of joints after test. No joint failure was observed in the AFLD implying the fact that applying AFLD to space structures will not impose failure mechanism related to joint instability. In the case of load carrying capacity, AFLD’s behavior is considerably prominent. As to compare with the

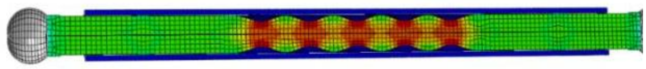

Fig. 12 Finite element model of AFLD

FLD tested by Parke (1988) which reached the ultimate load of 340 kN, our test scale AFLD could reach the same load range (310 kN) though it was smaller in length (approximately one third of the mentioned FLD’s length). Therefore, AFLD made in larger sizes to be used in actual structures is certainly more capable in reaching higher levels of load carrying capacity compared with FLD. To justify this point, we resort to the load carrying capacity of AFLDs with different sizes. Comparing the load carrying capacity of first and second test specimens (Figs. 8 and 10-a) reveals that by increasing AFLD’s size (in terms of length and diameter), the load carrying capacity increases. In the following, results obtained from experimental study of second specimen are used for verification of finite element modeling.

5. Finite element modeling

In the present study, the finite element modeling of the all steel accordion force limiting device was developed using ABAQUS finite element software. The experimental force-displacement response of second test specimen was used to evaluate the validity of the finite element modeling.

5.1 Description of modeling

The model includes accordion core, encasing and Mero-like joint system (as shown in Fig. 12). The ABAQUS/ Standard was used for the AFLD modeling.

Material properties for encasing and core were selected according to results of coupon tests (Tables 2-3). Mero-like joint was modeled as discrete rigid part due to heat treatment process applied on it; however core and encasing were modeled using solid elements. Static Riks analysis was performed to trace the equilibrium path through limit point into the post-critical range. The ‘Arc-Length-Type Method’ has been used. Contact properties of tangential coulomb frictional behavior were assumed between core and encasing. According to Genna’s research (Genna and Gelfie 2012) friction coefficient of 0.15 was used for lubricated steel to steel interface. Separation of core and encasing was allowed after contact, however the penetration was not allowed. Screw connection between the core and spherical joint was simulated with the tie connection of ABAQUS to increase the analysis efficiency. Both spherical joints, acted as pin joints. Despite the fact that end connections are set to be pinned, presence of moment in joints is possible due to AFLD’s imperfection. In modeling AFLD, imperfection of $L_c/1000$ was applied to the middle of AFLD. Having applied the imperfection, the behavior of AFLD is realistic concerning the presence of moment in both ends. It is obvious that the realistic behavior of AFLD will lead to the realistic behavior of structure. Displacement boundary conditions for the joint at the right side of core (which is fixed in the downward grip as shown in Fig. 6-b) were set to be zero. Another joint could freely move along the longitudinal axis of core and compression force was applied on top of it. In order to let the core part undergo large plastic deformations, C3D20 element was used. As mentioned earlier in describing the AFLD, core was a solid shaft. Therefore solid elements were used for modeling the core. Regarding the encasing, it is worth noting that for a hollow tube if the ratio of tube diameter to tube thickness, D_e/t, is less than 20, then solid elements is recommended for modeling the tube (Sadowski and Rotter (2013)). In all the models of this study (including the models used to verify the experimental tests and the models in parametric study) the ratio of tube thickness to tube radius was, D_e/t, less than 20. Accordingly, for modeling the encasing C3D8R elements were used. Mesh sensitivity analysis was carried out in order to find the appropriate mesh size for each model. An initial curvature with maximum lateral deflection amount of $L_c/1000$ (L_c is the core length) was applied to the middle of core as an imperfection shape. It is to be mentioned that force reversal can occur in space structure members including AFLDs, thus these members may go into tension. When applying AFLD behavior to the modeling of space structures, both tension and compression behaviors of AFLD should be introduced to the model. In this case, the analysis will follow the tension or compression behavior depending on the type of force in AFLD.

5.2 Verification

The axial force-axial displacement response of finite element model in comparison with the experimental results obtained for the second test specimen is shown in Fig. 13. Having carried out the mesh sensitivity analyses for this model, mesh size for Mero joint, core and encasing was set to be 2.5mm, 4mm and 4mm, respectively. It can be seen from this figure that the numerical behavior predicted by nonlinear finite element analysis closely follows the actual behavior exhibited by the experimental specimen. Consequently, it has been found that the developed finite element model is reliable enough to be used for undertaking nonlinear analyses of parametric study. To further explain the discrepancies between the experimental and finite element results, especially focusing on the discrepancy seen along the BC line (shown in Fig. 13) in numerical and experimental results, we may refer to the friction coefficient in numerical study. By increasing load, plastic hinges extend along the core, as shown in Fig. 14-b. In this point, core hits encasing which leads to increasing of load carrying capacity from point B to C (see Figs. 13 and 14-c). This notion is coincident with the LVDT results presented in the experimental part (see Fig. 11). These results highlight the further validity of finite element modeling of AFLD.

6. Parametric study

In order to evaluate the behavior of AFLD for improving the performance of space structures, a parametric study has been carried out. The force-displacement behavior, load carrying capacity, displacement ductility ratio and dissipated energy have been considered in the evaluation of AFLD's behavior. Accordingly, nine AFLD models were designed in full scale and modeled in ABAQUS software. Having carried out the mesh sensitivity analyses, mesh size for Mero joint, core and encasing was set to be 3mm, 10mm and 10 mm, respectively. This parametric study covers the following parameters: Effect of core material, Effect of accordion wave length, Effect of accordion diameter.

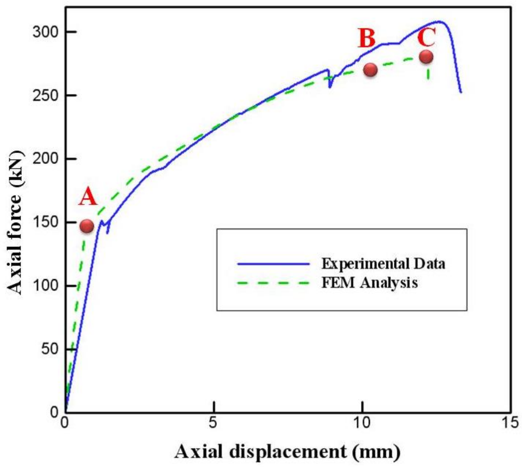

Fig. 13 Comparison of numerical and experimental axial force-axial displacement responses for second test specimen. Points A, B and C indicate the key behavior points of AFLD

6.1 Effect of core material

In order to evaluate the effect of core material on the behavior of AFLD, three full scale models were designed and developed in ABAQUS finite element software. In these models (Models 1-3), encasing was modeled as a tube of length 1600 mm with its outer and inner diameter being 89 and 70 mm, respectively. The gap between core and encasing was assumed to be 1.5 mm. Inner diameter of accordion, outer diameter of accordion and core diameter were assumed to be 50 mm, 67 mm, and 67 mm, respectively. The accordion wave length was assumed to be 120 mm, leading to an accordion including 10 waves. As an important parameter to control the AFLD's behavior, core material was selected based on the material properties given in Table 4. Stress-strain relationship of these materials (CK45, ST37 and ST52) is presented in Fig. 15. Effect of core material on AFLD's behavior in terms of axial force-axial displacement is presented in Fig. 16-a. In this figure, vertical axis stands for the applied axial force and horizontal axis presents the displacement measured in top of spherical joint. Fig. 17 presents the stress countors of models 1-3. As expected, core material has a considerable effect on the performance of AFLD. It is shown that by increasing the yield stress and ultimate stress of core material, load carrying capacity as well as ultimate axial displacement of AFLD significantly improves.

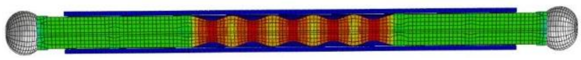

(a)

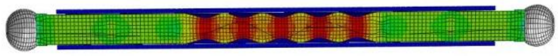

(b)

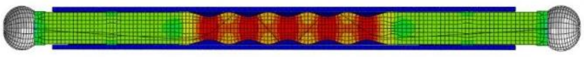

(c)

Fig. 14 Stress countors of model: (a) in point A, (b) in point b, (c) in point c as indicated in Fig. 13

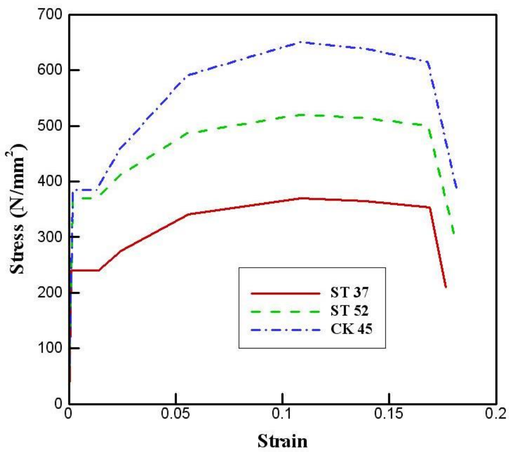

Fig. 15 Stress-strain relationship for ST37, ST52 and CK45

To investigate the effect of core material on AFLD's deformability, displacement ductility ratio (ratio of deformation in ultimate load to displacement in yield stress) is presented in Table 5. These data show that ductility ratio is highly affected by core material. By increasing the ultimate strength of material, ductility ratio increases enabling AFLD to undergo larger deformations without collapsing. Post-elastic behavior of AFLD is totally controlled by yield stress and ultimate stress of core material. The ability of AFLD to dissipate energy was also measured. As stated in Table 5, dissipated energy increases by increasing the yield stress and ultimate stress of core material (models 1-3). These results suggest that core material is an influential parameter in AFLD's behavior. Therefore, due to architectural limitations, selecting an appropriate core material is the best solution for obtaining the desired load carrying capacity in AFLDs. Elastic stiffness of device is related to the elastic modulus of the core material. Accordingly, for studying the effect of elastic modulus of core on the AFLD behavior, two different steel grades with different elastic modulus values of 165 and 205 GPa have been used for the core material (model 4 and model 5). Properties of model 4 and model 5 are given in Table 4. Dimensions of model 4 and model 5 are the same as model 1. Effect of elastic modulus of core material on the axial force-axial displacement response of AFLD is shown in Fig. 16-b. The behavior of model 1 is also included in the figure as a reference to compare the results. The slope of the OA line (shown in Fig. 16-b) can be a representative of

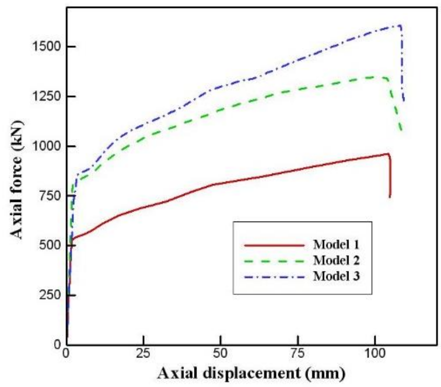

(a)

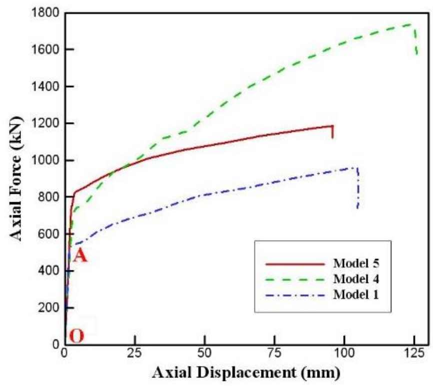

(b)

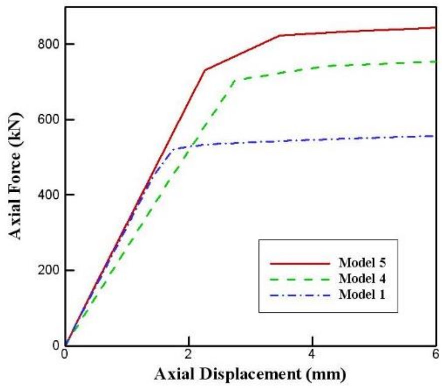

(c)

Fig. 16 Effect of core material on the axial force-axial displacement behavior of AFLD; (a) Effect of yield stress and ultimate stress, (b) Effect of elastic stiffness, (c) Zoomed plot of Fig. 16-b

(a)

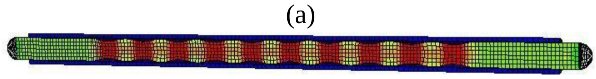

(b)

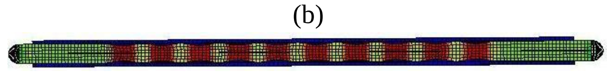

(c)

Fig. 17 Stress countors addressing the effect of core material: (a) Model 1, (b) Model 2, (c) Model 3

device's elastic stiffness. To focus on the results, the zoomed plot of Fig. 16-b is depicted in Fig. 16-c. As shown in this figure, the slope of curves (of the OA line) corresponding to model 5 and model 1 are approximately the same, due to the fact that their elastic modulus are close to each other. However the slope of model 4 differs from these two models due to the difference in elastic modulus. Results highlight that elastic modulus of core material affects AFLD's elastic stiffness. By increasing the elastic modulus of core material, elastic stiffness of AFLD increases. The difference shown in this figure from point A to the end of curve is definitely due to the difference between yield stress and ultimate stress of models, as mentioned in results of Fig. 16-a.

6.2 Effect of accordion wave length

The core of AFLD, as the most important element of AFLD, can influence its behavior significantly. In order to investigate the effect of wave length as an important factor in the design of core, three AFLD models with different accordion wave lengths (150 mm, 200 mm, and 300 mm) were developed in ABAQUS finite element software. The core material was selected to be CK45 and general dimensions of these models were considered to be the same as model 1. Properties of models 6, 7, 8 and the corresponding comparative results are given in Table 6. Effect of accordion wave length on the axial force-axial displacement response of AFLD is shown in Fig. 18-a, which demonstrates that by decreasing the accordion wave length (increasing the number of waves), plastic deformation is increased.

Stress countors of models 6-8 are also presented in Fig. 19, addressing the formation of plastic hinges. According to the data of Table 6, It has been found that by increasing the wave length for a given core length, values of ductility ratio, dissipated energy and ultimate load carrying capacity decrease. To justify this finding, we resort to the accordion shape effect. By increasing the wave length, core's accordion shape tends toward a simple bar, thus eliminating the positive effects caused by core's accordion shape due to the formation of plastic hinges. To further investigate the effect of accordion shape on AFLD behavior, response of AFLD with regular core (simple shaft) is also included in Fig. 18-a. It is evident from this figure that AFLDs equipped with accordion shaped core reach to higher levels of load carrying capacity, while the AFLD with simple core (model 9) has the minimum load carrying capacity amongst models. It is to emphasize that, accordion shape significantly improves the behavior of AFLD from the viewpoint of load carrying capacity.

6.3 Effect of accordion diameter

The accordion diameter is another important factor influencing the performance of AFLD. To investigate the effect of this parameter, the outer diameter of accordion core was assumed to be fixed due to the architectural limitations while the inner diameter of accordion core was set to be 44 mm, 40 mm and 36 mm in models 10, 11 and 12, respectively. Effect of inner diameter of accordion on the axial force-axial displacement responses of AFLD is shown in Fig. 18-b, indicating that by decreasing the inner diameter, load carrying capacity decreases due to the decreasing of loading surface. The models 10, 11, 12 and the related stress countors are shown in Fig. 20. Properties and comparative results for these models are given in Table 7. It can be found that by decreasing the inner diameter of core, the values of ductility ratio, dissipated energy and ultimate load carrying capacity decrease.

Table 4 Material properties of models 1- 5

Model no.	Core material	Yield stress	Ultimate stress	Elastic Stiffness
		(MPa)	(MPa)	(GPa)
1	ST37	240	370	200
2	ST52	360	520	200
3	CK45	385	650	200
4	316L	332	673	165
5	AISI 1018	370	440	205

Table 5 Comparative results of models 1-5

Model no.	Core material	Ultimate load carrying capacity	Ductility ratio	Dissipated energy
		(kN)		(J)
1	ST37	958	51.12	76856
2	ST52	1341	52.1	107737
3	CK45	1606	53.24	131610
4	316L	1768	85.3	156433
5	AISI 1018	1181	40.7	94290

Table 6 Comparative results of models 6-9

Model no.	Wave length	Ultimate load carrying capacity	Ductility ratio	Dissipated energy
	(mm)	(kN)		(J)
6	150	1622	41.2	127565
7	200	1522.5	33.04	98106
8	300	1393	27.6	70039
9	No waves	970	26.65877	47660

Table 7 Comparative results of models 10-12

Model no.	Core inner diameter	Ultimate load carrying capacity	Ductility ratio	Dissipated energy
	(mm)	(kN)		(J)
10	44	1319	32.22	84387
11	40	1118	22.09	59325
12	36	926	18.43	39922

7. Algorithm for designing AFLD

AFLDs can significantly improve the behavior of space structures by preventing the buckling of compression members. Therefore, an applicable design algorithm for

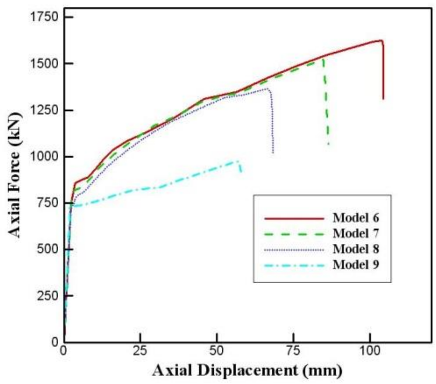

(a)

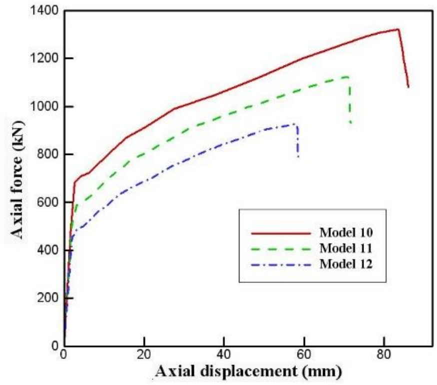

(b)

Fig. 18 Effect of accordion geometry on the axial force-axial displacement behavior of AFLD; (a) effect of accordion wave length, (b) accordion inner diameter

(a)

(b)

(c)

Fig. 19 Stress countors addressing the effect of wave length: (a) Model 6, (b) Model 7, (c) Model 8

(a)

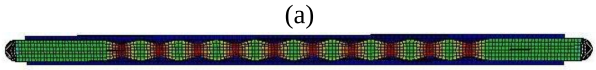

(b)

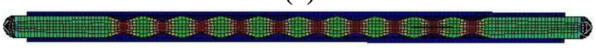

(c)

Fig. 20 Stress countors addressing the effect of accordion core diameter: (a) Model 10, (b) Model 11, (c) Model 12

predicting AFLD's behavior is presented. The considered assumptions in this algorithm are assumed to be: (1) Encasing prevents core from global buckling; (2) Friction between core and encasing is negligible; (3) Supports at two ends of core (joints) are assumed to be hinged; (4) Gap

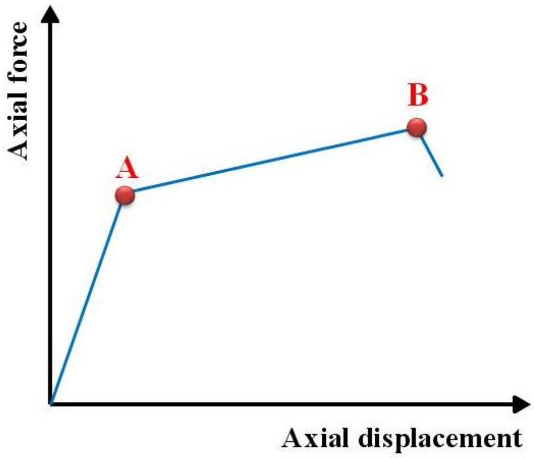

Fig. 21 Determinative points in designing AFLD (shown by red dots named A and B)

between core and encasing is set to have a limited value, say 1-2 mm; (5) Uniaxial compression load is applied. The main determinative points affecting the response of AFLD are shown in Fig. 21 (points A and B). Point A refers to the onset of plastic hinge formation. Subsequently, curve continues to reach point B where AFLD collapses. The possible range for axial force in point A is predicted as follows:

$$F_{\alpha} = \alpha A_{min}\sigma_y \tag{5}$$

Where, F_A is the axial load in point A, σ_y is the yield stress of core material, A_{min} is the cross sectional area corresponding to the inner diameter of accordion and α stands for the accordion shape coefficient as a factor related to the accordion's curvature. This coefficient is considered to be one for a plain bar while its value increases by increasing the accordion's curvature which can be improved by increasing the number of waves or decreasing the inner diameter of accordion. Core shape coefficient was set to be 1.25 for the presented experimental test specimen and values smaller than 1.25 are used in the numerical models. According to experimental and numerical results, the range of 1-1.25 is suggested to be used for accordion core coefficient. However, more investigation is required to accurately define this value. The possible range for axial force in point B is estimated as follows:

$$F = \alpha\beta A_{min}\sigma_u \tag{6}$$

In which, F_B is the axial load in point B, σ_u is the ultimate stress of core material. Cross sectional area and accordion shape factor (as introduced earlier) are shown by A_{min} and α, respectively. β is a factor related to ability of encasing to prevent global core buckling. According to the numerical and experimental results, the value of β is suggested to be approximately in the range of 1-1.5.

8. Conclusion

A new type of FLD, namely, an "all steel accordion force limiting device" is introduced in the present paper.

AFLD is an innovative force limiting device, which is designed inspired by the structural configuration of buckling restrained braces and accordion metallic damper. Designing an accordion core for the force limiting device as well as equipping the device with encasing is the novelty of the proposed AFLD. The main objective of the present study was to see if by applying AFLD it is possible to control the buckling of space structures' members. To this end, two all steel AFLD specimens were designed and manufactured to be tested under uniaxial compressive loading. The experimental results obtained from uniaxial compression test reveal that it is indeed possible to alter the brittle post-buckling behavior of normal members to elastic-perfect plastic behavior. Finite element modeling of AFLD was developed and verified with the results of experimental tests. Geometric and material nonlinear finite element analyses were carried out to conduct parametric study covering the effects of core material, accordion diameter and accordion wave length. Finally a procedure for predicting AFLD's axial force-axial displacement behavior was presented enabling one to control the force-displacement characteristics. Main findings of the present study are as follows:

- Comparison of obtained experimental results with the available data in technical literature showed that (i) AFLD's performance in controlling the buckling phenomenon was much efficient than previous FLDs; (ii) AFLD reached a higher level of load carrying capacity in comparison with the usual FLDs; (iii) The proposed system is easy to build and simple to assemble and disassemble which facilitates the replacing of damaged parts of AFLD with new ones.
- Numerical results suggest that (i) core material has a more dramatic effect on AFLD's behavior as compared with other parameters; (ii) utilizing a core material with high values of yield stress and ultimate stress improves AFLD's behavior, its ductility and dissipated energy; (iii) elastic modulus of core material does affect AFLD's elastic stiffness; (iv) by increasing the wave length for a given core length, values of ductility ratio, dissipated energy and ultimate load carrying capacity decrease; (v) by decreasing the inner diameter of core, the values of ductility ratio, dissipated energy and ultimate load carrying capacity decrease.
- The experimental and numerical results obtained in this study can be of significance in space structures dealing with buckling issues, suggesting that AFLD is an advantageous method to improve the behavior of space structure due to its efficient performance in improving the behavior of compression members as well as its simple design, ease of fabrication and assembling.

References

ABAQUS User's Manual (2010), Dassault Systèmes Simulia Corp., Providence, RI, U.S.A.

Bai, L. and Zhang, Y. (2012), "Collapse fragility assessment of steel roof framings with force limiting devices under transient wind loading", *Frontiers Struct. Civil Eng.,* **6**(3), 199-209. https://doi.org/10.1007/s11709-012-0168-4.

Bai, L. and Zhang, Y. (2013), "Nonlinear dynamic behavior of steel framed roof structure with self-centering members under extreme transient wind load", *Eng. Struct.,* **49**, 819-830. https://doi.org/10.1016/j.engstruct.2012.11.005.

Beiraghi, H. (2017), "Earthquake effects on the energy demand of tall reinforced concrete walls with buckling-restrained brace outriggers", *Struct. Eng. Mech.,* **63**(4), 521-536. https://doi.org/ 10.12989/sem.2017.63.4.521.

Chou, C. C., Chung, P. T. and Cheng, Y. T. (2016), "Experimental evaluation of large-scale dual-core self-centering braces and sandwiched buckling-restrained braces", *Eng. Struct.,* **116**, 12-25. https://doi.org/10.1016/j.engstruct.2016.02.030.

DIN 50125, Testing of metallic materials - Tensile test pieces.

El-sheikh, A. (1999), "Effect of force limiting devices on behavior of space trusses", *Eng. Struct.,* **21**(1), 34-44. https://doi.org/10.1016/s0141-0296(97)00136-3.

Genna, F. and Gelfi, P. (2012), "Analysis of the lateral thrust in bolted steel buckling restrained braces. I: Experimental and numerical results", *J. Struct. Eng.*, **138**(10), 1231-1243. https://doi.org/10.1061/(asce)st.1943-541x.0000558.

Gere, J.M. and Goodno, B.J. (2012), *Mechanics of Materials*, (8th edition), Cengage Learning, CA, U.S.A.

Hanaor, A., Marsh, C. and Parke, G.A.R. (1989), "Modification of behavior of double-layer Grids: Overview", *J. Struct. Division (ASCE),* **115**(5), 1021-1037. https://doi.org/10.1061/(asce)0733-9445(1989)115:5(1021).

Hanaor, A. and Schmidt, L.C. (1980), "Space truss studies with force limiting devices", *J. Struct. Division (ASCE),* **106**(11), 2313-2329.

Hemmati, S. Barkhordare Bafghi, M.A. and Kheyroddin, A. (2018), "Experimental investigation of pod on the behavior of all-steel buckling restrained braces", *J. Construct. Steel Res.,* **150**, 186-194. https://doi.org/10.1016/j.jcsr.2018.08.010.

Hosseinipour, S.J. and Daneshi, G.H. (2003), "Energy absorption and mean crushing load of thin-walled grooved tubes under axial compression," *Thin Wall Struct.*, **41**, 31-46. https://doi.org/10.1016/s0263-8231(02)00099-x.

Mirtaheri, M., Sehat, S. and Nazeryan, M. (2018), "Improving the behavior of buckling restrained braces through obtaining optimum steel core length", *Struct. Eng. Mech.*, **65**(4), 401-408. https://doi.org/10.12989/sem.2018.65.4.401.

Motamedi, M. and Nateghi, A.F. (2018), "Study on mechanical characteristics of accordion metallic damper", *J. Construct. Steel Res.,* **142**, 68-77. https://doi.org/10.1016/j.jcsr.2017.12.010.

Mukai, H., Wada, A., Watanabe, A., and Iwata, M. (1993), "Ductile truss structures and scaled model experiment", *Proceedings of the Fourth International Conference on Space Structures*, Surrey, United Kingdom, September.

Nooshin, H. (1998), "Space structures and configuration processing", *Progress Struct. Eng. Mater.*, **1**, 329-336.

Pandikkadavath, M.S. and Sahoo, D. R. (2015), "Ductility demand on reduced-length buckling restrained braces in braced frames", *Adv. Struct. Eng.,* **43**(1), 48-57. https://doi.org/10.1007/978-81-322-2187-6_180.

Parke, G.A.R. (1988), "The behavior of space trusses incorporating novel compression members", Ph.D. Dissertation, University of Surrey, United Kingdom.

Sadowski, A, J. and Rotter, J. M., (2013), "Solid or shell finite elements to model thick cylindrical tubes and shells under global bending", *J. Mech. Sci.*, **74**, 143-153. https://doi.org/10.1016/j.ijmecsci.2013.05.008.

Schmidt, L. C. and Hanaor, A., (1980), "Force limiting devices in space trusses", *J. Struct. Division (ASCE)*, **105**(5), 939-951.

Schmidt, L. C., Morgan, P. R. and Clarkson, J. A. (1976), "Space trusses with brittle type strut buckling", *J. Struct. Division (ASCE)*, **112**(7), 1479-1492.

Shekastehband, B. (2018), "The influences of force-limiting devices and high-stiffness cables on behavior of tensegrity structures", *Arch. Appl. Mech.*, **88** (12), 2293-2316. https://doi.org/10.1007/s00419-018-1455-x.

Tada, M. and Wakiyama, K. (1993), "Load-carrying capacity of space trusses under the influence of imperfections", *Proceedings of the Fourth International Conference on Space Structures*, Surrey, UK, September. https://doi.org/10.1680/ss4v1.19683.0022.

Thornton, Ch. and Lew, I. P. (1984), "Investigation of the causes of Hartford Coliseum collapse", *Proceedings of the Third International Conference on Space Structures*, Guildford, UK.

Watanabe, A., Hitomi, Y., Yaeki, E., Wada, A. and Fujimoto, M. (1988), "Properties of brace encased in buckling-restraining concrete and steel tube", *Proceedings of the 9th World Conference on Earthquake Engineering*, Tokyo, Japan.

Xie, Q. (2005), "State of the art of buckling-restrained braces in Asia", *J. Construct. Steel Res.*, **61**, 727-748. https://doi.org/10.1016/j.jcsr.2004.11.005.

CC